Internal modes and magnon scattering on topological solitons in two-dimensional easy-axis ferromagnets

Denis D. Sheka,[1,*] Boris A. Ivanov,[2] and Franz G. Mertens[1]
[1]*Physikalisches Institut, Universität Bayreuth, D-95440 Bayreuth, Germany*
[2]*Institute of Magnetism, NASU, 03142 Kiev, Ukraine*
(Received 12 January 2001; published 22 June 2001)

We study the magnon modes in the presence of a topological soliton in a two-dimensional Heisenberg easy-axis ferromagnet. The problem of magnon scattering on the soliton with arbitrary relation between the soliton radius R and the ''magnetic length'' Δ_0 is investigated for partial modes with different values of the azimuthal quantum numbers m. Truly local modes are shown to be present for all values of m, when the soliton radius is large enough. The eigenfrequencies of such internal modes are calculated analytically on the limiting case of a large soliton radius and numerically for arbitrary soliton radius. It is demonstrated that the model of an isotropic magnet, which admits an exact analytical investigation, is not adequate even for the limit of small radius solitons, $R \ll \Delta_0$: there exists a local mode with nonzero frequency. We use the data of local modes to derive the effective equation of soliton motion; this equation has the usual Newtonian form in contrast to the case of the easy-plane ferromagnet. The effective mass of the soliton is found.

DOI: 10.1103/PhysRevB.64.024432 PACS number(s): 75.10.Hk, 75.30.Ds, 75.70.Kw

I. INTRODUCTION

Nonlinear topologically nontrivial excitations (solitons) are well known to play a special role in low dimensional magnetic systems. For example, the presence of vortices in two-dimensional (2D) easy-plane (EP) magnets gives rise to the Berezinskiĭ-Kosterlitz-Thouless (BKT) phase transition.[1,2] Kinks in 1D magnets and localized Belavin-Polyakov (BP) solitons[3] in 2D isotropic magnets are responsible for the destruction of long-range order at finite temperature. The soliton signatures in dynamical response functions can be observed experimentally. Translational motion of solitons leads to the so-called soliton central peak.[5–7] Another possibility to detect soliton signature is to look for magnon modes, localized at the soliton [*local modes* (LM)]; such modes are the cause of soliton magnetic resonance at the characteristic frequencies of ''intrinsic'' motion.[8]

This can be explained within the scope of the so-called soliton phenomenology, where the magnet can be described as a two-component gas of elementary excitations: solitons and magnons. Such an approach was developed for 1D magnets.[4] It was shown that the contribution of magnons and soliton-magnon interaction is important for this approach, as is obvious, for example, in the discussion of soliton magnetic resonance.[4] But for 1D magnets the soliton-magnon scattering causes a change of the magnon density of states, which is necessary for a self-consistent calculation of the temperature dependence of the soliton density.[4]

For the 2D case, the concept of a soliton (vortex) gas has been extended to describe EP magnets above the BKT vortex-antivortex unbinding transition, with a finite density of vortices.[9,10] The concept of localized topological solitons (π_2-topological solitons, see details in Ref. 11) was used to explain the EPR linewidth in easy-axis (EA) magnets.[12–18] The classical example of a localized soliton is BP solution, which exists in isotropic magnets. The scattering problem for such solitons allows an exact analytical solution because of the scale and conformal invariance of the model.[19,20] For EA magnets it is necessary to take account of some important modifications due to the breaking of such symmetries. That is why, both for EA and EP 2D magnets, the soliton density has not been calculated, but has been used as an input parameter. The general features of the 2D soliton dynamics are not clear at present. In particular, the form of inertial terms in the dynamical equations for the soliton center is unknown; so the study of localized states is an issue of current research. Note that the problem of the soliton dynamics and the problem of the existence of LM are intimately connected to each other, and to the problem of soliton-magnon scattering. For example, using numerical data for the scattering amplitude, a non-Newtonian effective equation of motion of the magnetic vortex was constructed.[21]

Usually non-1D solitons and, especially, the problem of soliton-magnon scattering, are treated numerically.[21–23] The exceptions are the analytical study of the scattering problem for EA and EP ferromagnets (FM) in the frameworks of the Born approximation.[24,25] However, such an approach is not adequate for the problem with nonsmall soliton-magnon interaction. Therefore it leads in Ref. 25 to the k dependence of the scattering amplitude, which differ strongly from the accurate result.[21] Recently the analytical investigation of the scattering problem has been done for the case of purely isotropic magnets, with the exact BP solution.[26,27,19] In particular, it was found that a soliton has a number of local modes of zero frequency;[26] such modes determine the main features of the scattering picture.[19] However, even a small uniaxial anisotropy leads to principal changes. Truly local modes (in contrast to quasilocal ones, below) with nonzero frequencies were found numerically in Ref. 28 for the soliton in EA FM for some special values of the azimuthal quantum number m; namely the mode with $m=-1$ for the soliton with the topological charge $q=1$, and the mode with $m=2$ for $q=2$ were investigated. It is natural that such local modes can not be found in the Born approximation, treated in Ref. 24. Note that local modes do not exist for the models of easy-plane

and isotropic ferromagnets, where the magnon spectrum has a gapless dispersion law. The case of the 2D EP antiferromagnet is an exception; for this model a finite–frequency, truly localized internal mode with $m=0$ exists inside the continuum spectrum.[29]

Recently there has also been renewed attention to the internal dynamics of the soliton. It is caused by the studying of small ferromagnetic particles in the so-called vortex state (magnetic dots). Magnetic dots are micron-sized magnetic samples, placed on a nonmagnetic substrate; they have different shapes: circular, quadratic, etc. The magnetic dots are interesting for the usage in the high-density magnetic storage devices[30,31] and from a fundamental point of view. As the dots are rather large (the size of magnetic dot exceeds the critical size of a single domain), their ground state could be inhomogeneous. Such a dot in the vortex state contains a magnetic singularity in the center of the vortex, or the Belavin-Polyakov soliton type.[32] The discrete magnon modes were observed for the uniformly magnetized dots by a resonance technique;[33] their theory was constructed using the Landau-Lifshitz equations.[34]

In this paper we consider the magnon modes which exist in 2D Heisenberg EA FM with a topological soliton. The model of an easy-axis ferromagnet is presented in Sec. II. An approximate solution for the soliton structure is examined. In Sec. III we formulate equations, describing magnons and solitons. In Sec. IV truly local magnon modes are calculated analytically by variational approach for the limiting cases of large and small radius solitons, and numerically for arbitrary radii. In Sec. V the problem of soliton-magnon scattering is formulated and treated numerically for different partial modes. The phenomenology of a pseudopotential is proposed in Sec. VI to analyze analytically both local states and the scattering problem. In Sec. VII we use results for local modes to derive the equations of soliton motion. Such equations are of Newtonian type (with the account of gyroscopic force), in contrast to both the case of the BP soliton in the isotropic magnet[19] and the case of the vortex in the EP magnet.[21] In the framework of this equation the soliton effective mass is calculated. A discussion and concluding remarks are presented in Sec. VIII.

II. MODEL AND ELEMENTARY EXCITATIONS

The dynamics of the classical ferromagnet is described by the Landau-Lifshitz equations for the normalized magnetization $\boldsymbol{m}$. In angular variables, $m_x+im_y=\sin\theta\exp(i\phi)$, these equations correspond to the Lagrangian

$$L=A\int d^2x\left\{\frac{1}{D}(1-\cos\theta)\frac{\partial\phi}{\partial t}-\mathcal{W}(\theta,\phi)\right\} \tag{1}$$

with the energy density $A\cdot\mathcal{W}(\theta,\phi)$,

$$\mathcal{W}(\theta,\phi)=\frac{1}{2}(\nabla\theta)^2+\frac{1}{2}(\nabla\phi)^2\sin^2\theta+\frac{1}{2\Delta_0^2}\sin^2\theta, \tag{2}$$

where $A=JS^2$, J is the exchange integral, S the atomic spin, $\Delta_0=\sqrt{A/K}$ the characteristic scale (''magnetic length''), K the energy of the anisotropy, and D the spin-wave stiffness.

The model of EA FM has well-known magnon excitations $\theta=\text{const}\ll 1$, $\phi=\omega t-\boldsymbol{k}\cdot\boldsymbol{r}$ above the homogeneous ground state. The dispersion law for the magnons has a finite activation frequency $\omega_0=D/\Delta_0^2$,

$$\omega(\boldsymbol{k})=\omega_0+D|\boldsymbol{k}|^2, \tag{3}$$

where $\boldsymbol{k}$ is the wave vector.

The simplest nonlinear excitation in the system is the dynamical (precessional) topological soliton[11]

$$\phi=\varphi_0+q\chi+\Omega t,\quad \theta=\theta_0(r),\quad \theta_0(0)=\pi,\quad \theta_0(\infty)=0, \tag{4}$$

where r and χ are polar coordinates in the plane of the magnet, the integer q plays the role of a topological charge, and Ω $(0<\Omega<\omega_0)$ is the frequency of the internal precession. The necessity to consider solitons with internal precession is caused by the fact that, according to the Derrick-Hobart theorem, static solitons in models like Eq. (2) are unstable. Formally, there is no function $\theta_0(r)$, which could provide a minimum of the energy

$$E=\pi A\int_0^\infty r dr\left\{\left(\frac{d\theta_0}{dr}\right)^2+\sin^2\theta_0\left(\frac{1}{\Delta_0^2}+\frac{q^2}{r^2}\right)\right\}. \tag{5}$$

The precessional soliton corresponds to the conditional minimum of the energy (5) for a given number N of magnons bound in the soliton

$$N=\frac{N_2}{\Delta_0^2}\int_0^\infty r dr[1-\cos\theta_0(r)], \tag{6}$$

which is conserved for the uniaxial case ($N_2=2\pi A/\hbar\omega_0$ is the characteristic number of bound magnons in the 2D soliton),[36] see also Refs. 11 and 35. This corresponds to the condition $\delta[E-N\hbar\Omega]=0$. The form of the function $\theta_0(r)$ is defined by the ordinary differential equation

$$\frac{d^2\theta_0}{dr^2}+\frac{1}{r}\frac{d\theta_0}{dr}-\sin\theta_0\cos\theta_0\left(\frac{1}{\Delta_0^2}+\frac{q^2}{r^2}\right)+\frac{\Omega}{\omega_0\Delta_0^2}\sin\theta_0=0, \tag{7}$$

with the boundary conditions (4). The precession frequency Ω is fully determined by the number of bound magnons N. The dependence $\Omega(N)$ was calculated numerically in Ref. 36; large radius solitons ($N\gg N_2$) have a very low precession frequency ($\Omega\ll\omega_0$), and $\Omega\to\omega_0$ for small radius solitons ($N\ll N_2$).

In the case of large radius solitons, $R\gg\Delta_0$, the approximate ''domain-wall'' solution[11]

$$\cos\theta_0(r)=\tanh\frac{r-R}{\Delta_0} \tag{8}$$

is applicable, which describes a 1D domain wall at the distance R from the origin. One can obtain the relation between the soliton radius R and the frequency of the soliton preces-

TABLE I. Fitting of the trial solution (10) to the exact numerical solution for $\theta_0(r)$. The radius of the soliton is defined from the condition $\theta_0(R)=\pi/2$.

Frequency of precession, Ω/ω_0	Soliton radius, R/Δ_0	Fitting parameter, $R^{(\mathrm{fit})}/\Delta_0$	Std. error, $\times 10^{-2}$
0.05	20.38	20.38	0.6
0.10	9.95	9.94	1.2
0.15	6.58	6.58	1.9
0.20	4.88	4.87	2.6
0.25	3.82	3.81	3.2
0.30	3.09	3.07	3.6
0.40	2.07	2.07	4.0
0.50	1.35	1.37	3.8
0.60	0.81	0.85	3.2
0.70	0.42	0.44	2.2
0.80	0.15	0.16	1.1
0.85	0.07	0.07	0.9

sion Ω from variational condition, in which R plays the role of a fitting parameter for the function (8). In the first approximation $\Omega(R)\approx\omega_0\cdot\Delta_0/R$.

The opposite case of small radius solitons, $R\ll\Delta_0$, corresponds to the Belavin-Polyakov solution $\tan(\theta_0/2)=(R/r)^{|q|}$, which describes the isotropic limit of the model (1); it is valid for distances $r\ll\Delta_0$.[3] At larger distances the algebraic decay is replaced by the general exponential form,

$$\theta_0(r)\propto\exp(-r/r_0),\quad r_0=\sqrt{\frac{D}{\omega_0-\Omega}}. \tag{9}$$

The dependence $\Omega(R)$ was calculated both analytically and numerically in Refs. 36 and 37. The frequency of the soliton precession satisfies $\Omega\to\omega_0$ when $R\to 0$, but the dependence $\Omega(N)$ is not analytic, and $d\Omega/dN\to\infty$ as $N/N_2\to 0$.[36]

To describe approximately the soliton structure in the intermediate case of arbitrary R, we use a fitting method.[38] We choose a trial function of the form

$$\tan\frac{\theta_0^{(\mathrm{fit})}(r)}{2}=\frac{R^{(\mathrm{fit})}}{r}\cdot\exp\left[-\frac{(r-R^{(\mathrm{fit})})}{r_0}\right], \tag{10}$$

which has valid asymptotics for $r\to 0$ and $r\to\infty$ (we discuss the case $q=1$ only). The parameter $R^{(\mathrm{fit})}$ can be found numerically by fitting the trial function (10) to the numerical solution of Eq. (7). Such an approximation shows that the trial function describes the soliton shape with an accuracy of about 10^{-2}, see Table I. From this table one can see that the values of the fitting parameter $R^{(\mathrm{fit})}$ are very close to the ''exact'' soliton radii; it should be understood by the fact that $\theta_0(r=R^{(\mathrm{fit})})=\pi/2$. Numerical data for $\theta_0(r)$ and fitting results for $\theta_0^{(\mathrm{fit})}(r)$ are plotted in Fig. 1.

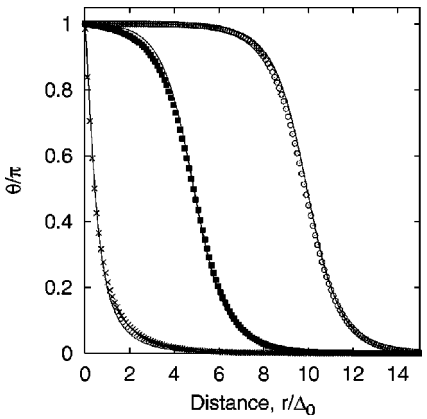

FIG. 1. Shape of $\theta_0(r)$ for different soliton radii R/Δ_0 ($\times=0.4$, $\blacksquare=5$, $\odot=10$). Lines: numerical data, symbols: fitting data with the trial function (10).

III. MAGNON MODES

To analyze magnons on the soliton background, it is convenient to introduce local coordinates $\{\boldsymbol{e}_1,\boldsymbol{e}_2,\boldsymbol{e}_3\}$, which describe the configuration of the magnetization unit vector $\boldsymbol{m}$ in the unperturbed soliton: $\boldsymbol{e}_3$ coincides with $\boldsymbol{m}$ in the soliton (4), $\boldsymbol{e}_1=\boldsymbol{e}_y\cos\phi_0-\boldsymbol{e}_x\sin\phi_0$, and $\boldsymbol{e}_2=\boldsymbol{e}_3\times\boldsymbol{e}_1$. Then the linear oscillations around the soliton can be described in terms of projections of the magnetization $\boldsymbol{m}$ on the local axes: $\mu=\boldsymbol{m}\cdot\boldsymbol{e}_1$ and $\vartheta=-\boldsymbol{m}\cdot\boldsymbol{e}_2$. In the absence of the soliton, $\theta_0=0$, $\phi_0=\Omega t$, such oscillations correspond to free magnons in the rotating coordinate frame.

The linearized equations for ϑ and μ can be presented in the form

$$[-\nabla^2+\mathcal{U}_1(r)]\vartheta+\frac{2q\cos\theta_0}{r^2}\frac{\partial\mu}{\partial\chi}=\frac{1}{\omega_0\Delta_0^2}\frac{\partial\mu}{\partial t}, \tag{11a}$$

$$[-\nabla^2+\mathcal{U}_2(r)]\mu-\frac{2q\cos\theta_0}{r^2}\frac{\partial\vartheta}{\partial\chi}=-\frac{1}{\omega_0\Delta_0^2}\frac{\partial\vartheta}{\partial t} \tag{11b}$$

with the ''potentials''

$$\mathcal{U}_1(r)=\left(\frac{1}{\Delta_0^2}+\frac{q^2}{r^2}\right)\cos 2\theta_0(r)-\frac{\Omega}{\omega_0\Delta_0^2}\cos\theta_0(r), \tag{12a}$$

$$\begin{aligned}\mathcal{U}_2(r)&=-\left(\frac{d\theta_0(r)}{dr}\right)^2+\cot\theta_0(r)\nabla_r^2\theta_0\\&=-\left(\frac{d\theta_0(r)}{dr}\right)^2+\left(\frac{1}{\Delta_0^2}+\frac{q^2}{r^2}\right)\cos^2\theta_0(r)\\&\quad-\frac{\Omega}{\omega_0\Delta_0^2}\cos\theta_0(r),\end{aligned} \tag{12b}$$

where ∇_r^2 is the radial part of the Laplace operator.

It is convenient to represent the solutions of Eqs. (11) in terms of a partial-wave expansion for ϑ and μ,

$$\vartheta=\sum_\alpha\,[u_\alpha(r)+v_\alpha(r)]\cos(m\chi+\tilde{\omega}_\alpha t), \tag{13a}$$

$$\mu = \sum_{\alpha} [u_{\alpha}(r) - v_{\alpha}(r)] \sin(m\chi + \tilde{\omega}_{\alpha} t), \qquad (13b)$$

where $\alpha = (k,m)$ is a full set of eigennumbers, k and m being radial and azimuthal quantum numbers, respectively. The quantity $\tilde{\omega} = \omega - \Omega$ is the magnon frequency in the rotating frame; k and $\tilde{\omega}$ are connected by the dispersion law, cf. Eq. (3),

$$\tilde{\omega}(\boldsymbol{k}) = \omega_{\rm gap} + D|\boldsymbol{k}|^2, \quad \omega_{\rm gap} = \omega_0 - \Omega, \qquad (3')$$

where $\omega_{\rm gap}$ is the magnon gap frequency in the rotating frame. Below we will replace $\tilde{\omega}$ by ω, almost everywhere without confusion, because we will work in the rotating frame mainly; the index α will be omitted, too. Thus we then finally obtain the following eigenvalue problem (EVP) for the functions u and v:

$$\hat{H}_1 u \equiv \left[\hat{H}_0 + \frac{m^2}{r^2} + V(r) - \frac{\omega}{\omega_0 \Delta_0^2} \right] u = W(r) v, \qquad (14a)$$

$$\hat{H}_2 u \equiv \left[\hat{H}_0 + \frac{m^2}{r^2} - V(r) + \frac{\omega}{\omega_0 \Delta_0^2} \right] v = W(r) u, \qquad (14b)$$

where $\hat{H}_0 = -\nabla_r^2 + U_0(r)$ is the 2D radial Schrödinger operator; the ''potentials'' are

$$U_0(r) = \frac{1}{2}(\mathcal{U}_1 + \mathcal{U}_2), \quad V(r) = \frac{2qm\cos\theta_0}{r^2}. \qquad (15a)$$

Note, that Eqs. (15) are invariant under the conjugations $\omega \to -\omega$, $m \to -m$, and $u \leftrightarrow v$. In a classical theory we can choose any sign of the frequency; but in order to make contact with quantum theory, with a positive frequency and energy $\mathcal{E}_k = \hbar|\omega_k|$, we will discuss the case $\omega > 0$ only. Thus there are two different sets of Eqs. (14) for $m = |n|$ and $m = -|n|$. Besides, there appears a difference between Eqs. (14a) and (14b). Since Eq. (14b) has the asymptotically equivalent form, $-\nabla_r^2 v + \omega v = 0$, the function v has an exponential behavior; at the same time Eq. (14a) yields oscillating solutions. So, by choosing $\omega > 0$, the variable v becomes a slave variable in the EVP (14).

The ''coupling potential'' W,

$$W(r) = \frac{1}{2}(\mathcal{U}_2 - \mathcal{U}_1) = \frac{1}{2}\left[\sin^2\theta_0 \left(\frac{1}{\Delta_0^2} + \frac{1}{r^2} \right) - \left(\frac{d\theta_0}{dr} \right)^2 \right], \qquad (15b)$$

is positive, it has a maximum value at a distance of about the soliton radius R from the origin, vanishing both at $r = 0$ and far from the soliton. Using the domain-wall approximation (8), one obtains that the maximum value of $W \propto 1/R^2$, when $R \gg \Delta_0$. In the opposite case of small R, in the range $r \ll R$ the soliton looks like the Belavin-Polyakov solution; here $r(d\theta_0/dr) \approx -\sin\theta_0$, and $W = 0$ in the main exchange approximation.[19] Therefore one can suppose that $W \ll 1/\Delta_0^2$ for any R. In fact, this is confirmed by numerical calculations, see Fig. 2.

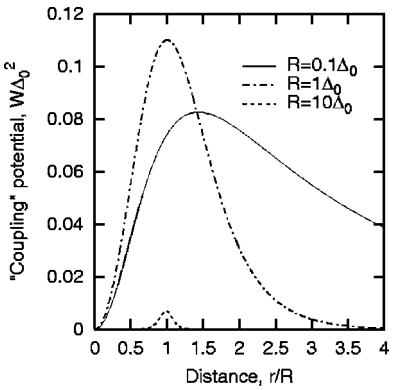

FIG. 2. Shape of the ''coupling'' potential for different soliton radii.

However, one can see below in Sec. IV that the problem is impoverished when the ''coupling potential'' $W(r)$ is ignored; even in the limits of small (large) soliton radii, the main properties of local modes vanish, if we assume that $W(r) = 0$. The reason is that a set of more than one coupled Schrödinger-like equations has properties, which are absent from a single equation. To explain this fact, remember that for a single 1D Schrödinger equation there exist two independent solutions; for the eigenfrequencies inside the continuous spectrum such solutions have oscillating asymptotics. For a set of 2, 3, ... equations there exist 4, 6, ... linearly independent solutions, respectively; some of them can have exponential asymptotics. Naturally, the real modes have an oscillational form here; we will use this fact below for the numerical analysis. But it is necessary to take into account the exponential solutions, too. In particular, as was shown in Ref. 29, such exponential asymptotics could correspond to truly localized states inside the continuous spectrum, which are forbidden for equations of the Schrödinger form. In the reduced EVP with two independent equations like Eq. (14) with $W = 0$, there is a continuous spectrum $\omega > \omega_{\rm gap}$ for the function $u(r)$ ($u \neq 0$, $v = 0$) and $\omega < -\omega_{\rm gap}$ for the function $v(r)$ ($u = 0$, $v \neq 0$). There are no limitations for the lowest value of the discrete levels; in particular, the frequencies of the discrete spectrum could be less than $-\omega_{\rm gap}$ for the function u. At the same time, as follows from the general set of coupled Eqs. (14), frequencies of local modes lie in the region $-\omega_{\rm gap} < \omega < \omega_{\rm gap}$. Therefore it is necessary to solve the general EVP (14) for an exact analysis of the problem.

We should note here that the model of an isotropic magnet is a special case, in which the ''coupling'' potential is exactly equal to zero. To study an EVP like Eq. (15) with $W = 0$, it is sufficient to take into account one equation only (namely, the equation for the variable u); the second one, which has unphysical solutions for $\omega > 0$, was ignored in Ref. 19. That is why the results for EA FM, obtained in this paper, and the results for the isotropic magnet[19] differ strongly even for small anisotropy. One difference is caused by the presence of truly local modes. Another one is due to the peculiar structure of the quasicontinuous spectrum with $\omega > \omega_{\rm gap}$ for a finite geometry: the spectrum of the EA FM

has a system of doublets with opposite signs of m, while there are no doublets for the isotropic magnet.

IV. LOCAL MODES

According to the dispersion law $(3')$, free magnons only exist when $\omega > \omega_{\rm gap}$. It is naturally to look for local modes in the range $0 < \omega < \omega_{\rm gap}$ (remember that we discuss the case $\omega > 0$). In principle, such local modes could exist inside the continuous spectrum, as for the case of the nonlinear σ model, describing the EP antiferromagnet.[29] However, our study shows that this is not the case for the EA FM. Existence of local modes in such a magnet was found numerically in Ref. 28 for a soliton with some special parameters; namely the mode with $m=-1$ for the soliton with the topological charge $q=1$, and the mode with $m=2$ for $q=2$ were calculated. Such modes appear in field theories, which include solitonlike solutions.[20]

To study local modes, note that near the soliton center, $r \ll \Delta_0$, one can obtain the asymptotics of the magnon amplitudes in the following form:

$$u_m(r) = \mathcal{A}_m \left(\frac{r}{\Delta_0}\right)^{|q-m|} [1 + O(r^2/\Delta_0^2)], \qquad (16a)$$

$$v_m(r) = \varepsilon \mathcal{A}_m \left(\frac{r}{\Delta_0}\right)^{|q+m|} [1 + O(r^2/\Delta_0^2)]. \qquad (16b)$$

Here the coefficient $\mathcal{A}$ can be determined by the normalization; the presence of a nonzero factor ε is caused by the ''interaction'' $W(r)$ between Eqs. (14a) and (14b); its value cannot be found through this asymptotic expansion.

In the opposite case of large distance, $r \gg \Delta_0$, the EVP (14) has the following general solution (here and below we consider the most interesting case of solitons with unit topological charge $q=1$, which has lowest energy):

$$u_m(r) \approx A_m K_{|m+1|}(\varkappa_1^- r) + B_m I_{|m+1|}(\varkappa_1^- r), \qquad (17a)$$

$$v_m(r) \approx C_m K_{|m-1|}(\varkappa_1^+ r) + D_m I_{|m-1|}(\varkappa_1^+ r), \qquad (17b)$$

where K_ν and I_ν are Macdonald and modified Bessel functions, respectively, and $\varkappa_1^\pm = \sqrt{(\omega_0 - \Omega \pm \omega)/D}$. Note that at large distances, $z \gg 1$, the modified Bessel functions have exponential behavior, $I_\nu(z) \propto \exp(z)/\sqrt{z}$, $K_\nu(z) \propto \exp(-z)/\sqrt{z}$, so we use the asymptotical condition $u_m, v_m \propto \exp(-\varkappa_1^\pm r)/\sqrt{r}$ to obtain the localized solutions.

First note that for the special cases $m=0,+1$ there exist ''zero modes'' with $\omega=0$. Such modes are caused by the internal symmetry of the problem. They have the same form as for EP magnets.[21] One of the zero modes, the so-called translational mode with $m=+1$,

$$u_{+1} = \frac{d\theta_0}{dr} - \frac{\sin\theta_0}{r}, \quad v_{+1} = \frac{d\theta_0}{dr} + \frac{\sin\theta_0}{r}, \qquad (18a)$$

describes the position shift of the soliton. Another one with $m=0$,

$$u_0 = \sin\theta_0, \quad v_0 = -\sin\theta_0, \qquad (18b)$$

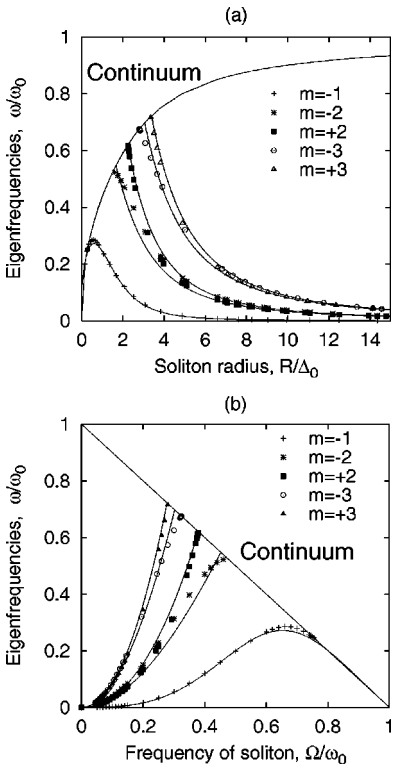

FIG. 3. Eigenfrequencies of local modes as functions of (a) soliton radius and (b) frequency of internal precession of the soliton. Lines: theoretical results from Eqs. (23b) and (27); symbols: numerical data.

is a rotational mode, which corresponds to the presence of an arbitrary parameter, the phase φ_0, in the soliton structure (4). For the isotropic magnet, as well as for the EP magnet, similar modes exist, too; but there they are quasilocal due to their slow power-law decay, $1/r$, or $1/r^2$. In the EA magnets the decay has an exponential form.

The remaining modes could be investigated numerically; analytical results were obtained for some limiting cases only, see below. To study the EVP numerically, we use the two-parameter shooting method for the integration of the set of Eqs. (14); a similar one-parameter shooting scheme was proposed in Ref. 29 to study the vortex-magnon scattering problem in 2D antiferromagnets. Numerically, we ''kill'' two growing exponents in Eqs. (17) by choosing two shooting parameters ε and ω. As a result, we have found numerically that there are a number of local modes. Modes with opposite signs of m bind to doublets; this picture is well pronounced for $|m|>1$ in the limit of large R, see Fig. 3.

Such local modes exist only for not too small soliton radii (not for large Ω). Eigenfrequencies for such modes with arbitrary azimuthal numbers m ($|m|>1$) increase rapidly with the decreasing of the soliton radius, and reach the boundary of the continuous spectrum. It looks as if all such modes ''leave'' the region of the gap in the spectrum, if the soliton radius is smaller than some critical value $R_m^{\rm c}$, see Table II. It is natural to suppose that all modes with $|m|>1$ transform to the quasilocal ones with decreasing of R; this fact can be tested numerically due to the singularities of the scattering amplitudes on such quasilocal modes, see the next section.

TABLE II. Critical parameters for some lower modes with $|m|>1$. Remember that local modes always exist for $m=0,\pm 1$.

m	R_m^c/Δ_0, data	Ω_m^c/ω_0, data	Ω_m^c/ω_0, from Eq. (24)
-2	1.52	0.47	0.45
$+2$	2.24	0.38	0.38
-3	2.73	0.33	0.30
$+3$	3.22	0.29	0.28

Thus in the range $R \lesssim 1.52\Delta_0$ there is only one local mode with nonzero frequency, $m=-1$, see Fig. 3. That is why only the mode with $m=-1$ was observed in Ref. 28 for the soliton with $q=1$.

The eigenfunctions of bound states u and v are localized near the soliton core. The functions u and v are plotted in Fig. 4 for the mode with $m=-1$; the picture of well-localized eigenfunctions is specially pronounced for the large radius solitons, see Fig. 4(a).

In order to analyze the spectrum of local modes analytically, let us reformulate the EVP (14) as a variational problem for the functional

$$F[u,v]=\int_0^\infty r dr(u\hat{H}_1 u+v\hat{H}_2 v-2Wuv). \qquad (19)$$

We start with large radius solitons, $R \gg \Delta_0$, when the domain-wall approximation (8) is valid. In the region of interest, $r \simeq R \gg \Delta_0$, the operator $\hat{H}_0$ from the EVP (14) has in the main approximation for Δ_0/R a simple reflectionless potential,

$$\hat{H}_0 \approx \hat{L} \equiv -\frac{d^2}{dr^2}+\frac{1}{\Delta_0^2}\left[1-\frac{2}{\cosh^2[(r-R)/\Delta_0]}\right]$$

with a single localized state ψ_0, corresponding to the zeroth eigenvalue

$$\hat{L}\psi_0=0, \quad \psi_0(r)=(2R\Delta_0)^{-1/2}/\cosh[(r-R)/\Delta_0].$$

The other potentials in the EVP can be considered as corrections to $\hat{L}$; this is the reason to put the trial functions in the form $u=a\psi_0$, $v=b\psi_0$ with trial parameters a and b. The variational approach with such simple trial functions leads to eigenfrequencies for the different modes in the form

$$\omega_m=m\alpha+\sqrt{(m^2\beta-\delta)^2-\gamma^2},$$

$$\alpha=\left\langle \psi_0\left|\frac{2\cos\theta_0(r)}{r^2}\right|\psi_0\right\rangle, \quad \beta=\left\langle \psi_0\left|\frac{1}{r^2}\right|\psi_0\right\rangle,$$

$$\gamma=\langle\psi_0|W(r)|\psi_0\rangle, \quad \delta=\left\langle \psi_0\left|\frac{1}{r}\frac{d}{dr}+\Omega\cos\theta_0(r)\right|\psi_0\right\rangle, \qquad (20)$$

where $\langle\psi_0|\cdots|\psi_0\rangle=\int_0^\infty\psi_0(\cdots)\psi_0 r dr$. However, there is a difference between the real solutions u, v, and the trial function ψ_0. This difference provides, e.g., the existence of ''zero modes.'' We do not like to improve the form of the eigenfunctions, but only the coefficients in the Eqs. (20), which describe the eigenfrequencies. Using the additional condition for zero modes,

$$\omega_m=0 \quad \text{for } m=0,+1, \qquad (21)$$

the eigenfrequencies ω_m can be expressed through two independent coefficients only. It is convenient to present the eigenfrequencies in the form

$$\omega_m=m\alpha+|m|\sqrt{\alpha^2+\beta^2(m^2-1)}. \qquad (22)$$

Using trial functions ψ_0, we can calculate the parameters α and β for the large radius solitons,

$$\alpha=-\omega_0(\Delta_0/R)^3, \quad \beta=\omega_0(\Delta_0/R)^2. \qquad (23a)$$

In this case the spectrum has the form

$$\frac{\omega_m}{\omega_0}=|m|\sqrt{\left(\frac{\Delta_0}{R}\right)^6+\frac{m^2-1}{(R/\Delta_0)^4}}-m\left(\frac{\Delta_0}{R}\right)^3 \qquad (23b)$$

This formula corresponds very well to the numerical data for $R \gg \Delta_0$, see Fig. 3. In the main approximation for Δ_0/R there is a system of doublets (for all modes with $|m|>1$) with quadratic dependence of the mean frequency on Δ_0/R,

$$\overline{\omega}_{\pm m}\approx\omega_0|m|\sqrt{m^2-1}\left(\frac{\Delta_0}{R}\right)^2, \qquad (23c)$$

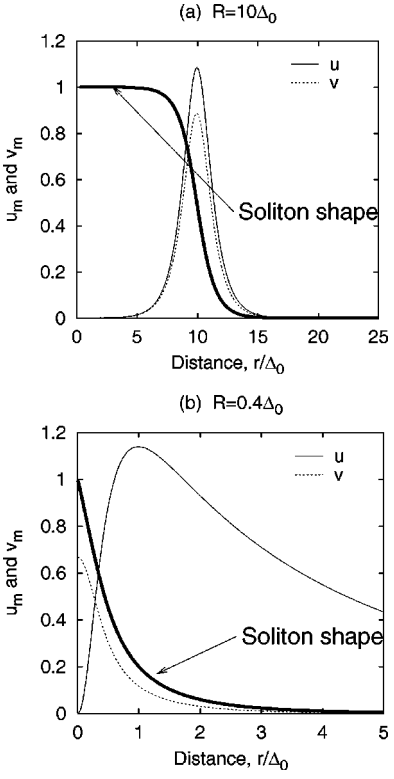

FIG. 4. Magnon amplitudes for local modes with $m=-1$.

and the splitting is a small cubic correction, $\Delta\omega_{\pm m} \propto m(\Delta_0/R)^3$. For the special case $m=-1$ the dependence $\omega(R)$ has the form

$$\omega_{m=-1} \approx 2\omega_0 \left(\frac{\Delta_0}{R}\right)^3. \tag{23d}$$

Equation (24b) describes qualitatively all modes with arbitrary R. In particular, it describes the fact, mentioned above, that modes reach the boundary of the continuous spectrum at some finite frequency of the soliton precession Ω_m^c. Let us estimate the positions of the crossover points, where the modes ''leave'' the discrete spectrum. Using Eq. (23b), one can obtain the condition for the critical values of $x=\Omega_m^c/\omega_0$:

$$|m|\sqrt{x^6+(m^2-1)x^4}-mx^3=1-x. \tag{24}$$

Results are very close to the numerical data, see Table II. We expect that the local modes transform into the quasilocal ones inside the continuous spectrum; but their frequencies can still be described by the formula (23b), see Sec. VI.

For the small radius solitons, $R \ll \Delta_0$, there only exist local modes with $|m|=1$. Thus we will consider this case. Constructing the trial functions, one can suppose that they should be similar to the modes with $m=\pm 1$. Eigenfunctions for the translational zero mode, u_{+1} and v_{+1}, are well known, see Eq. (18a). To construct the trial functions it is convenient to use functions u_{-1} and v_{-1} in the form

$$u_{-1}=r^2u_{+1}, \quad v_{-1}=r^2v_{+1},$$

which coincide with the exact zero mode eigenfunctions for the mode with $m=-1$ in the limiting case of the BP soliton.[19] Now we can choose the trial functions u and v as follows:

$$u=a\cdot u_{+1}+b\cdot u_{-1}, \quad v=c\cdot v_{+1}+d\cdot v_{-1}. \tag{25}$$

The variational problem (19) can be solved analytically in the main approximation for R/Δ_0 using the explicit BP solutions. Tedious calculations lead to the eigenfrequency for small R,

$$\omega_{m=-1} \approx C\cdot(\omega_0-\Omega). \tag{26}$$

Unfortunately, this method is not exact and leads to a value of the constant C which is larger than the numerical value. This is caused by the fact that the trial functions, which are constructed from zero modes, have the wrong asymptotical behavior (9) at large distance, $\theta_0(r)$, $\theta_0'(r) \propto \exp(-r/r_0)$, instead of Eq. (17), i.e., $u \propto \exp(-\varkappa_1^- r)$, $v \propto \exp(-\varkappa_1^+ r)$. To improve this result, one can change the asymptotical behavior of the functions (25) by exponential factors:

$$u \to u\cdot e^{r(1/r_0-\varkappa_1^-)}, \quad v \to v\cdot e^{r(1/r_0-\varkappa_1^+)}.$$

In this case the calculations can be done numerically only; the value of the constant $C \approx 1$. For the approximate description of the eigenfrequency of the mode with $m=-1$ in the intermediate case of arbitrary R, we use the trial function

$$\omega_{m=-1}^{(trial)}(\zeta)=\omega_0\cdot\frac{2\zeta^3(1-\zeta)}{1-\zeta+2\zeta^4}, \quad \zeta=\frac{\Omega}{\omega_0}. \tag{27}$$

Providing the asymptotically correct behavior, Eqs. (23d) and (26), this approximation reproduces to the numerical results with an accuracy of about 2×10^{-3}, see Fig. 3.

V. SCATTERING PROBLEM: NUMERICAL RESULTS

Let us describe the scattering of magnons by a soliton. Note that without a soliton, free magnon modes have the form

$$u_m(r) \propto J_m(kr), \quad v_m(r)=0, \tag{28}$$

where k is a ''radial wave number,'' k and ω are connected by the dispersion law (3′), and J_m are Bessel functions. The free modes like u_m play the role of the partial cylinder waves of a plane spin wave

$$\exp(i\boldsymbol{k}\cdot\boldsymbol{r}-i\omega t)=\sum_{m=-\infty}^{\infty} i^m J_m(kr)e^{im\chi-i\omega t}. \tag{29}$$

To describe magnon solutions in the presence of a soliton, one should note that far from the soliton, $r \gg \Delta_0$, the ''coupling potential'' $W(r)$ is exponentially small. Therefore there are two asymptotically independent EVP's; the magnon amplitude v_m has the same form (17b) as for the local modes, but the function u_m shows an oscillating behavior like

$$u_m(r) \propto J_{|m+1|}(kr)+\sigma_m(k)Y_{|m+1|}(kr), \tag{30}$$

where $Y_{|m+1|}$ are Neumann functions. The quantity $\sigma(k)$ derives from the soliton-magnon scattering; it can be interpreted as the scattering amplitude.

We use the one-parameter shooting method to study numerically the problem of soliton-magnon scattering, as described in Ref. 29 for vortices in the antiferromagnet. Choosing the shooting parameter ε, see Eq. (16), we ''kill'' the growing exponent in Eq. (17b); as a result we have obtained a well-pronounced exponential decay for v_m; the corresponding oscillating solutions for u_m differ from the asymptotical values (30) only in the vicinity of the soliton core, see Fig. 5. The scattering amplitude was found from these data by comparison with the asymptotics (30). The results are the following:

For all modes the scattering amplitude $\sigma_m(k)$ tends to zero as $k \to 0$. In the long-wavelength limit the maximal scattering is related to the mode with $m=-1$, for which the behavior of $d\sigma/dk$ looks singular. However, other properties depend strongly on the soliton radius.

In the case of large R, the scattering amplitude $\sigma_m(k)$ is positive for all modes in the long-wavelength limit. There is a maximum of $\sigma_m(k)$ at about $kR \sim 1$ for modes with *positive m*; but there are two poles in the scattering amplitude for modes with *negative m*, and one pole for $m=0$. Naturally, there is no real divergence at such a pole: the physically observed phase of the scattering, or the phase shift δ_m

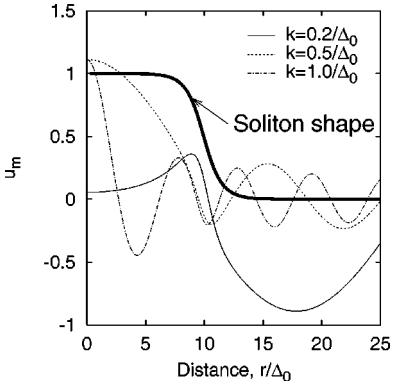

FIG. 5. Oscillating magnon amplitudes u_m for soliton with radius $R=10\Delta_0$ for different wave numbers k.

$=-\tan\sigma_m$, varies monotonically, see Fig. 6. Thus there are principally different pictures for positive and negative m: the total phase shift is

$$\delta_m^{tot} \equiv \delta(\infty) - \delta(0) = \begin{cases} 0, & m>0 \\ -\pi, & m=0, \\ -2\pi, & m<0 \end{cases} \quad R \gg \Delta_0 . \tag{31a}$$

The scattering picture is quite different for the case of small radius solitons. Each mode with $|m|>1$ has a single pole only, the position k_pR of which increases when m grows. For the special case of the mode with $m=+1$, the scattering amplitude is anomalously small; for the mode with $m=-1$ there appears a second pole with anomalously small values of k_p. These results are presented in Fig. 7. The total phase shift is

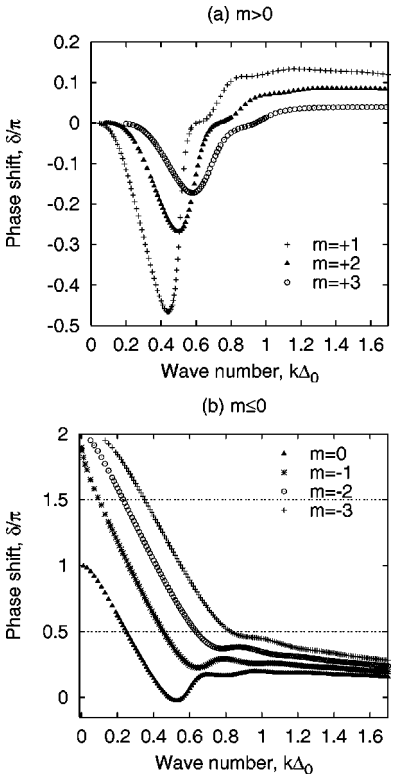

FIG. 6. Scattering for a large radius soliton, $R=10\Delta_0$. Numerical data.

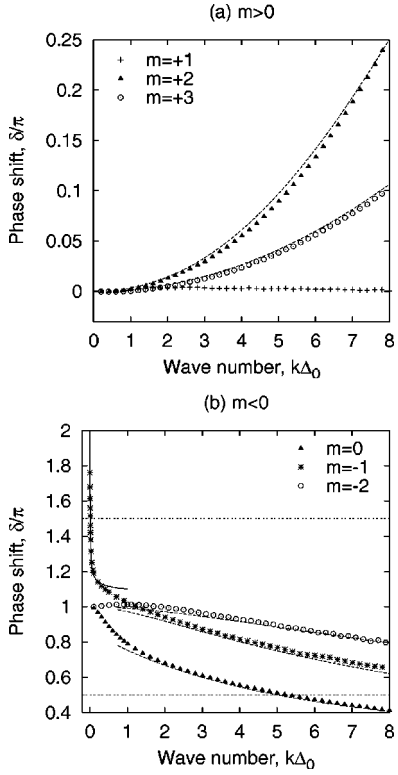

FIG. 7. Scattering for a small radius soliton, $R=0.2\Delta_0$. Solid line: analytical asymptotics for $k \ll 1/\Delta_0$ for the mode $m=-1$ from Eqs. (46a); dashed lines: analytical asymptotics for $k \gg 1/\Delta_0$ from Eqs. (38); symbols: numerical data.

$$\delta_m^{tot} = \begin{cases} +\pi, & m>1 \\ 0, & m=1 \\ -2\pi, & m=-1 \\ -\pi, & m=0, \quad m<-1 \end{cases} \qquad R \ll \Delta_0 . \tag{31b}$$

There appears a discontinuous change of the total phase shift from Eq. (31a) to Eq. (31b) for all modes with $m \neq 0$, -1 for the cases of intermediate soliton radii. This transition occurs independently for each mode at some critical values k_m^c of the wave number.

VI. SCATTERING PROBLEM IN THE FRAMEWORK OF THE PSEUDOPOTENTIAL METHOD

For the analytical description of the scattering problem, let us analyze the EVP qualitatively, replacing the real ''potentials'' (15) in the EVP (14) by simplified ones, which are amenable to an exact treatment. Such an approach is well known in the quantum physics of solids as the pseudopotential method. Sometimes it is useful even when the potential is not small, see Ref. 39 for details.

Let us discuss the choice of the pseudopotential. The simplest way is to describe the soliton structure in the main

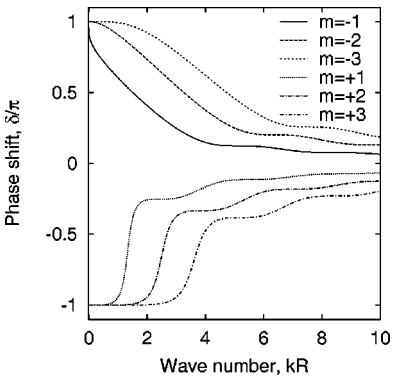

FIG. 8. Scattering for the centrifugal model.

approximation, using the ansatz

$$\cos\theta_0(r)\approx \mathrm{sgn}\ \xi, \quad \xi=\frac{r-R}{\Delta_0}, \tag{32}$$

which is a good approximation for both small and large distances. Replacing the soliton by this configuration, which does not have any in-plane structure ($\sin\theta_0=0$), reduces the complex EVP (14) to a very simple ''centrifugal model'' with $v_m\equiv 0$:

$$\left(-\nabla_r^2+k^2+\frac{|m+\mathrm{sgn}\ \xi|^2}{r^2}\right)u_m=0. \tag{33}$$

This model describes quasifree magnons in each of the regions $r<R$ and $r>R$. The only effect of the soliton–magnon interaction is a shift of the mode indexes in comparison with the free magnons (28):

$$u_m(r)\propto\begin{cases} J_{|m-1|}(kr), & r<R, \\ J_{|m+1|}(kr)+\sigma_m(k)Y_{|m+1|}(kr), & r>R. \end{cases} \tag{34}$$

The usual matching condition for these solutions has the form

$$\left[\frac{u'}{u}\right]_R=0, \tag{35}$$

where $[\cdots]_R\equiv(\cdots)|_{R+0}-(\cdots)|_{R-0}$. Calculations lead to the scattering amplitude in the form

$$\sigma(\varkappa)=\frac{J'_{|m-1|}(\varkappa)\cdot J_{|m+1|}(\varkappa)-J'_{|m+1|}(\varkappa)\cdot J_{|m-1|}(\varkappa)}{J_{|m-1|}(\varkappa)\cdot Y'_{|m+1|}(\varkappa)-J'_{|m-1|}(\varkappa)\cdot Y_{|m+1|}(\varkappa)}, \tag{36}$$

where $\varkappa=kR$, see Fig. 8. The total phase shift in this model is

$$\delta_m^{tot}=\pi\cdot\mathrm{sgn}\ m. \tag{37}$$

A. Small radius solitons, $R\ll\Delta_0$

The simple ''centrifugal model'' with the results (36) explains qualitatively the scattering data for the small radius solitons, except for modes with $m=0,\pm 1$, cf. Eq. (31b). The cause for these exceptions is the existence of truly local modes (''zero ones'' for $m=0,+1$, and another one with nonzero frequency for $m=-1$); while such modes are absent for the other m. The existence of a local mode diminishes the total phase shift by π (and decreases the number of states in the continuum spectrum by 1, due to the conserved total number of magnon states). Such a result is well known in 1D, see, e.g., Ref. 7. Except for these cases, one can expect for the scattering peculiarities at $k\sim 1/R\gg 1/\Delta_0$. In this range the approximation by an isotropic magnet and BP solitons is valid. The scattering problem for the isotropic magnets was studied in detail in Ref. 19. Over a wide range of wave numbers, $1/\Delta_0\ll k\ll 1/R$, the asymptotics for the Belavin-Polyakov soliton are valid,[19]

$$\sigma_{m\neq -1,0}(k)=-\frac{\pi(kR)^2}{2|m|(m+1)}, \tag{38a}$$

$$\sigma_{m=0}(k)=\frac{\pi}{2\ln(1/kR)}, \tag{38b}$$

$$\sigma_{m=-1}(k)=\pi(kR)^2\ln(1/kR). \tag{38c}$$

For larger wave numbers, $k\gg|m|/R$, the scattering amplitude has a general, so-called eikonal dependence, $\sigma_m\propto 1/kR$,[19]

$$\sigma_m(k)=\frac{\pi(m-1)}{kR}. \tag{38d}$$

Our numerical data in this region are very close to the asymptotical behavior (38), see Fig. 7. Note that the maximal scattering in the region $1/\Delta_0\ll k\ll 1/R$ occurs for the rotational mode with $m=0$, whose asymptotics (38b) has a singularity for $k\to 0$. There is one pole only for each mode; its position corresponds to the pole in the Belavin-Polyakov solution, $k_p\sim|m|/R$.[19]

Let us consider the local modes, for which the total phase shift is diminished by π in comparison to the ''centrifugal model'' (37); it is equal to 0, $-\pi$, -2π for the cases $m=+1$, 0, -1, respectively.

There is one pole only for the simplest case of the mode with $m=0$. The scattering amplitude in the range $1/\Delta_0\ll k\ll 1/R$ is described by the formula (38b). The position of the pole is determined by the BP result $k_p=1/R$.[19] The reason for such a nice agreement with the model of the isotropic magnet will be explained below in the text.

There is no pole for the translational mode with $m=+1$. This is due to a unique property of the isotropic model, where such a mode does not scatter at all;[19] the magnon amplitude in this limit has the form

$$u_{m=+1}(r)=J_2(kr)-\frac{2}{kr}\cdot\frac{J_1(kr)}{(r/R)^2+1}, \tag{39}$$

which agrees with our numerical data, see Fig. 9. This unique property of reflectionlessness is caused by the high internal symmetry of the problem.

Figure 7(a) shows that such a property is approximately valid for the small radius soliton in the anisotropic magnet, too: the scattering amplitude is anomalously small, so the

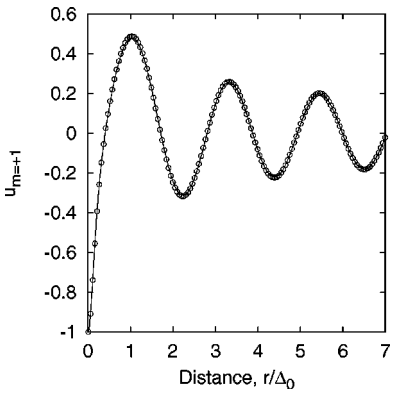

FIG. 9. Magnon amplitude u for the translational mode with $m=+1$ ($R=0.2\Delta_0$, $k\Delta_0=3$). Lines: exact analytical solution (39) for the isotropic magnet; symbols: numerical data for the EA FM.

total phase shift is absent. Another effect of this symmetry in the isotropic magnet is that the scattering problem for the BP model can be reduced to a simplified one with effectively smaller scattering. Such a ''reduced model'' has no local (and quasilocal) modes; it is described by shifted indexes, $m\to m-1$.[19] It is natural to use the ''centrifugal'' approximation for such a reduced model (36). As a result, $\sigma_{m=+1}=0$ in the framework of the same centrifugal model; for the other modes, Eq. (37) leads to the total phase shift $\delta_m^{tot}=\pi\cdot\mathrm{sgn}(m-1)$. Taking into account that $\mathrm{sgn}\,0=0$, one can see that such a simple dependence for δ_m^{tot} describes all modes, except of $m=-1$. Its behavior is most interesting.

For the mode with $m=-1$ there are two poles, while it should be one pole only for the Belavin-Polyakov solitons. Indeed, one of the poles lies in the region where the Belavin-Polyakov approximation is valid; its value, $k_p\approx 2.79/R \gg 1/\Delta_0$, coincides exactly with the Belavin-Polyakov data.[19] The second pole lies in the region $k\ll 1/\Delta_0$, where the approximation by the isotropic magnet is not applicable. This pole is caused by the presence of the local mode, the typical wave number of such a mechanism is $k_p\sim\varkappa_1^{\pm}\ll 1/\Delta_0$. The use of reduced or centrifugal models is certainly wrong for this case. We will discuss the scattering amplitude in this region later, on the basis of a more general pseudopotential model, see Eq. (46a).

B. Large radius solitons, $R\gg\Delta_0$: Refinement of the pseudopotential model

Let us consider the case of large radius solitons, $R\gg\Delta_0$. Here exist local modes for each m. Therefore the simple centrifugal model as well as other simple models without a discrete spectrum seem to be wrong. This can be explained by the fact that in the very simple model (33) we omit the ''coupling potential''; the real potential W tends to zero at the origin and at infinity, but has maxima at some finite distances.

Thus we need a more general form of the pseudopotentials which accounts for the potentials U_0, V, and W. To describe the soliton shape, we can again use the expression (32) for the out-of-plane soliton configuration. However, we need to consider the in-plane signature, too. According to Eq. (32), it could be described as

$$\sin^2\theta_0(r)\to\delta(\xi).$$

Therefore we can suppose that the coupling potential $W(r)$ is nonzero only at some distance around the soliton radius and approximately replace it by a δ potential as follows:

$$W(r)\to\frac{c_1}{\Delta_0^2}\delta(\xi). \tag{40a}$$

The same assumptions lead to simple expressions for the other potentials in the EVP (14),

$$U_0(r)+\frac{m^2}{r^2}\pm V(r)\to\frac{1-(\Omega/\omega_0)\cdot\mathrm{sgn}\ \xi}{\Delta_0^2}+\frac{|m\pm\mathrm{sgn}\,\xi|^2}{r^2}$$

$$+\frac{c_2}{\Delta_0^2}\delta(\xi). \tag{40b}$$

Here c_1 and c_2 are trial parameters.

We choose this pseudopotential model (40) for the following reasons: (i) it allows an exact analytical solution; (ii) it guarantees the correct asymptotic behavior of the solutions; (iii) it offers a possibility to identify the parameters of the pseudopotential from the discrete spectrum (23).

Let us consider the discrete spectrum in the framework of the pseudopotential (40). Comparison with the eigenfrequencies (23) provides a possibility to determine all trial parameters c_k. For the discrete part of the spectrum, the EVP (14) with potentials (40) has solutions like

$$u_m(r)\propto\begin{cases}I_{|m-1|}(\varkappa_2^- r), & r<R\\ K_{|m+1|}(\varkappa_1^- r), & r>R,\end{cases} \tag{41a}$$

$$v_m(r)\propto\begin{cases}I_{|m+1|}(\varkappa_2^+ r), & r<R\\ K_{|m-1|}(\varkappa_1^+ r), & r>R,\end{cases} \tag{41b}$$

$$\varkappa_1^{\pm}=\sqrt{(\omega_0-\Omega\pm\omega)/D},\quad \varkappa_2^{\pm}=\sqrt{(\omega_0+\Omega\pm\omega)/D}.$$

Now it is possible to calculate the eigenspectrum by matching the solutions (41a) and (41b) at the distance R,

$$[u']_R=\frac{c_2}{\Delta_0}\cdot u\Big|_R-\frac{c_1}{\Delta_0}\cdot v\Big|_R, \tag{42a}$$

$$[v']_R=\frac{c_2}{\Delta_0}\cdot v\Big|_R-\frac{c_1}{\Delta_0}\cdot u\Big|_R. \tag{42b}$$

Calculations lead to the eigenfrequencies in the form (20). Using the condition for the zero modes (21), the eigenfre-

quencies can be represented in the form (22); the constants c_1, c_2 can be identified by comparison with the spectrum (22),

$$c_1=\frac{1}{2}\left(\beta-\frac{\alpha^2}{\beta}\right),\quad c_2=-2+c_1+m\alpha+m^2\beta-\frac{\Delta_0^2}{4R^2}. \tag{43}$$

The parameters α and β were calculated by the variational approach, $\alpha\propto 1/R^3$, $\beta\propto 1/R^2$, see Eq. (23a).

Let us discuss the scattering problem. Solving the EVP (14) with pseudopotentials (40), we obtain for the continuum spectrum, $\omega>\omega_{\rm gap}$, the following solutions. The function u for $r<R$ has the form

$$u(r)\propto\begin{cases} I_{|m-1|}(\varkappa_2^- r), & \text{when } k<\sqrt{2\Omega/D},\\ J_{|m-1|}(k_2^- r), & \text{when } k>\sqrt{2\Omega/D},\end{cases} \tag{44}$$

where $k_2^-=\sqrt{k^2-2\Omega/D}$. At large distances, $r>R$, it has the usual oscillating form (30). The function v has the localized form (41b). One can find the scattering amplitude by matching the solutions (30), (44), and (41b) at the distance R, using the condition (42):

$$\sigma_m(k)=\frac{[\mathfrak{C}_m(k)+\mathfrak{F}_m(k)]J_{|m+1|}(kR)-k\Delta_0 J'_{|m+1|}(kR)}{k\Delta_0 Y'_{|m+1|}(kR)-[\mathfrak{C}_m(k)+\mathfrak{F}_m(k)]Y_{|m+1|}(kR)}, \tag{45}$$

here

$$\mathfrak{C}_m(k)=c_2-c_1^2\cdot\left(c_2+\varkappa_2^+\Delta_0\cdot\frac{I'_{|m+1|}(\varkappa_2^+R)}{I_{|m+1|}(\varkappa_2^+R)}-\varkappa_1^+\Delta_0\cdot\frac{K'_{|m-1|}(\varkappa_1^+R)}{K_{|m-1|}(\varkappa_1^+R)}\right)^{-1},$$

$$\mathfrak{F}_m(k)=\begin{cases}\varkappa_2^-\Delta_0\cdot\dfrac{I'_{|m-1|}(\varkappa_2^-R)}{I_{|m-1|}(\varkappa_2^-R)}, & k<\sqrt{2\Omega/D},\\[2ex] k_2^-\Delta_0\cdot\dfrac{J'_{|m-1|}(k_2^-R)}{J_{|m-1|}(k_2^-R)}, & k>\sqrt{2\Omega/D}.\end{cases}$$

It is easy to analyze the expression for the scattering amplitude (45) in some limiting cases. In the long-wavelength limit, $k\ll 1/R\ll 1/\Delta_0$, one can use the asymptotics for the cylindrical functions $J(z)$, $Y(z)$ at $z\ll 1$ and, at the same time, the asymptotics for $I(z)$, $K(z)$ for $z\gg 1$. Simple calculations show that the scattering intensity is maximal for the mode with $m=-1$,

$$\sigma_{m=-1}(k)=\frac{\pi}{2\ln(1/kR)},\quad kR\ll 1, \tag{46a}$$

which agrees with the numerical data, see Fig. 6(b). Note that Eq. (46a) was obtained using one condition only, $kR\to 0$. Therefore it is valid for the case of small R, too, explaining the existence of the second pole for the mode $m=-1$ both for large and small radii.

For the other values of m, we can restore the general dependence of the amplitude of the magnon scattering on the large radius soliton, $R\gg\Delta_0$:

$$\sigma_{m\neq -1}(k)=\frac{\pi(kR/2)^{2|m+1|}}{|m+1|!(|m+1|-1)!},\quad kR\ll 1. \tag{46b}$$

The scattering amplitude, according to Eq. (46b), is positive for all modes in the long-wavelength limit.

In the range $1/R\ll k\ll 1/\sqrt{R\Delta_0}$ the asymptotics for $J(z)$, $Y(z)$ for $z\gg 1$ are valid, which in the main approximation for Δ_0/R leads to a linear dependence of the scattering phase shift on kR,

$$\delta_m(k)\approx\frac{|m+1|\pi}{2}-\frac{\pi}{4}-kR,\quad 1\ll kR\ll\sqrt{\frac{R}{\Delta_0}}. \tag{46c}$$

For this range of k, all curves look like a family of parallel lines with equal distance of about $\pi/2$. Note that the real values of the trial parameters c_1 and c_2 lead to the corrections in Eqs. (46) like Δ_0/R.

Naturally the pseudopotential method cannot explain the scattering results for $k\gtrsim 1/\Delta_0$, where the influence of truly local modes and the differences between the real potential and the δ function are dominant. Nevertheless, the method gives quite good results even for the case $k\lesssim 1/\Delta_0$, where the linear asymptotics does not work. Corresponding curves are plotted in Fig. 10 using the general dependence (45) with trial parameters c_1 and c_2. Fitting of these parameters gives a result in the zeroth-order approach for Δ_0/R: $c_1\approx 0$, $c_2\approx 0.4$ instead of $c_1\approx 0$, $c_2\approx -2$, according to Eq. (43). The difference is caused by the limitations of the model (40). For example, the above-mentioned model leads to an increase of the scattering phase when k increases; the total phase shift for this model is $\delta_m^{tot}=\text{sgn}\, m\cdot\pi$, as for the centrifugal model, see Eq. (37), i.e., the qualitative properties of these models are equivalent. The appearance of a local mode diminishes the total phase shift by π. As a result, there is no total phase shift for all modes with positive m; but $\delta^{tot}=-2\pi$ for all modes with $m<0$.

The scattering picture in the short-wavelength limit, $k\gg|m|/R$, gives the general, so-called eikonal dependence $\sigma_m\approx A_m/k$. However, in contrast to the case of the isotropic magnet (38d), the scattering amplitude has the same sign $A_m<0$ for all modes due to the presence of the effective attractive potential, which causes the existence of local modes. When the soliton radius decreases and the local mode disappears, the sign of σ_m changes; the result becomes similar to Eq. (38d).

Thus we explain the particularities in the scattering picture of EA magnets, in comparison with the isotropic case, by the influence of local modes. To examine this influence, let us consider the scattering data σ_m for the modes $m=+2$ and $m=-2$ with different soliton radii R as functions of the parameter kR, i.e., $\sigma=\sigma_m(kR)$; this gives a possibility to compare the scattering data with the isotropic model, see Fig. 11. For the small radii the scattering picture is similar to the BP case (solid lines in Fig. 11). When the soliton radius

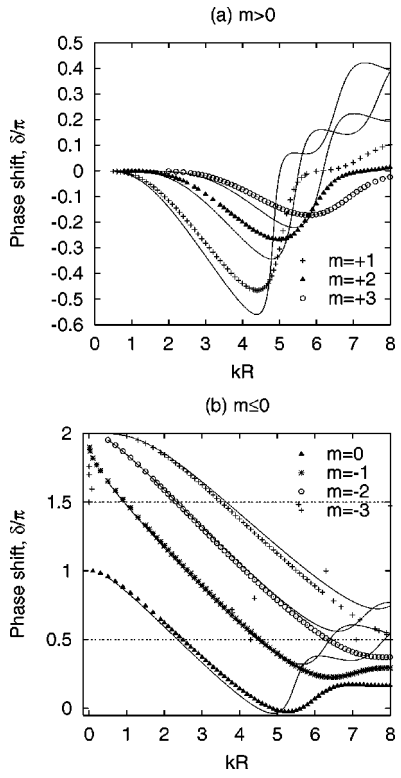

FIG. 10. Scattering amplitude δ_m for large radius soliton ($R=10\Delta_0$) vs kR in the range $k\Delta_0<0.8$. Lines: analytical solution from Eq. (45); symbols: numerical data.

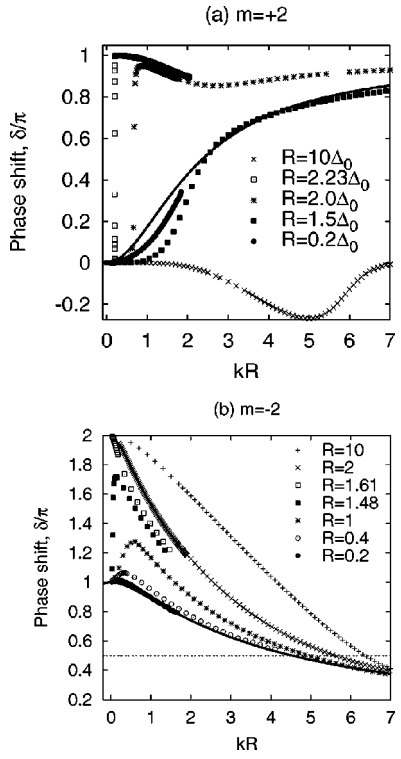

FIG. 11. Bifurcations for the scattering data δ_m vs kR: (a) critical soliton radius $R^c_{m=+2}=2.24\Delta_0$, (b) $R^c_{m=-2}=1.52\Delta_0$. Solid line corresponds to the Belavin-Polyakov asymptotics (38).

increases, the scattering phase jumps up by π, decreasing the total phase shift. Such a bifurcation takes place for the mode with $m=+2$ at $R=2.24\Delta_0$, and for the mode with $m=-1$ at $R=1.52\Delta_0$. These values agree with the crossover points R^c_m, see Table II. Thus it is natural to suppose that the bifurcation is connected with the appearance of the quasilocal modes inside the continuum spectrum for $R>R^c_m$. Simple calculations show that the positions k_p of the poles correspond to the frequencies of quasilocal modes, which can be estimated by Eq. (23b).

VII. TRANSLATIONAL MODES AND DESCRIPTION OF THE SOLITON DYNAMICS

The foregoing analysis of the spectrum for the modes with $|m|=1$ can be used to describe the translational motion of the soliton. Such an approach was proposed in Ref. 40, where an effective mass of the vortex in a 2D EP magnet was calculated from numerical data for the eigenmode spectrum of the finite-size magnet. Important progress for the vortices in FM was achieved in Ref. 21; the specific structure of the spectrum of modes with $|m|=1$ (namely the existence of a Goldstone mode with $\omega\propto 1/L^2$, and a number of doublets with mean frequency $\overline{\omega}\propto 1/L$ and a small splitting) leads to non-Newtonian equations of motion with 3rd, 5th, ... time derivatives. Such equations were derived and discussed earlier in Ref. 41, using a phenomenological approach, for a review see Ref. 42. The analytical calculation[21] verified their adequacy; besides, it allows to calculate the coefficients in the equations of motion with an error of only about 0.8%. Thus it is possible to describe in this way such unusual properties as the appearance of the non-Newtonian equations of motion.

The spectrum of magnon modes with $|m|=1$ has a different structure for the isotropic FM. First of all, there are no doublets;[19] for an approximate description of the dynamics only two modes are sufficient: the translational Goldstone mode with dependence $\omega\propto 1/L^2$ and another mode with $m=-1$. Therefore the effective equations of motion have a Newtonian form with an effective mass, which diverges as L^2, see Ref. 19. Such behavior agrees with the direct calculations done by Zaspel.[15]

Let us note that all magnets mentioned above, i.e., EP and isotropic systems, have a gapless dispersion law and, as a result, a strong interaction of the soliton with the boundaries of the magnet; the interaction force is proportional to $1/L$ for the EP vortices[21] and $1/L^2$ for the Belavin-Polyakov solitons.[19] The absence of a gap manifests itself in the particularities of the dynamical coefficients (the effective mass M for the BP soliton in the isotropic FM,[19] and the coefficient G_3 in the term with $[\boldsymbol{e}_z\times\partial^3\boldsymbol{X}/\partial t^3]$ for the vortex in the EP FM Ref. 41). This can be explained as follows. The existence of the mass M and the gyroscopical force $G[\boldsymbol{e}_z\times\partial\boldsymbol{X}/\partial t]$ leads to a finite frequency of the Larmor precession of the soliton. For a gapless dispersion law, this frequency lies in the continuous spectrum. Thus the Larmor motion of the vortex leads to the generation of magnons. For a finite-size system without dissipation, such magnons are distributed through the whole magnet; the Larmor dynamics

of the soliton center is strongly coupled with a ''magnon cloud,'' having a scale of about the system size. Therefore the position of the soliton center, which can be determined as a point with $m_z=-1$ (BP soliton), or $m_z=\pm 1$ (vortex), in fact plays the role of a collective variable which governs the motion of the magnon cloud. Then it is not surprising that the corresponding equations of motion are nonlocal, leading to the divergence of the dynamic coefficients as $L\to\infty$.

The situation is quite different for the case of the EA FM. Our numerical analysis and analytical calculations show that the picture of doublets for local modes with $|m|$ and $-|m|$ is valid for large R, see Sec. IV. On the other hand, the eigenfrequencies of these modes lie in the gap for the large soliton radii, $\omega<\omega_{\rm gap}$, so one can expect the existence of a finite mass in the effective equations of the soliton motion. Therefore for the phenomenological description of the soliton dynamics we can use the 2nd-order differential equation

$$M\frac{\partial^2 \boldsymbol{X}}{\partial t^2}-G\left[\boldsymbol{e}_z\times\frac{\partial \boldsymbol{X}}{\partial t}\right]=\boldsymbol{F}_e(\boldsymbol{X}), \tag{47}$$

which corresponds to the picture with the lowest doublet of local modes. Note that further generalizations for the finite-size magnet take into account the next doublets of quasicontinuous modes. Here the hierarchy of the effective equations of motion containing only even-order time derivatives manifests itself. In Eq. (47) $\boldsymbol{X}$ describes the position of the soliton, M is the mass coefficient, G the gyrocoefficient, $\boldsymbol{e}_z$ the unit vector along the easy (z) axis, and $\boldsymbol{F}_e$ the external force acting on the soliton due to the boundary or other solitons. Assuming that deviations of the soliton from the equilibrium position are small, $\boldsymbol{F}_e\approx-\alpha\boldsymbol{X}$, the effective equation of motion (47) can be solved by a harmonic ansatz, which leads to

$$\omega_{0,1}=\frac{G}{2M}\pm\sqrt{\frac{G^2}{4M^2}+\frac{\alpha}{M}}. \tag{48}$$

For the localized solitons, the interaction between soliton and boundary (or between two solitons) has an exponential decay as $\exp(-L/r_0)$, $r_0=\sqrt{D/\omega_{\rm gap}}$, see Eq. (9). Thus α/M can be neglected for a large system size L, so the frequencies (48) have the form

$$\omega_0=0,\quad \omega_1=G/M. \tag{49}$$

The zero frequency ω_0 corresponds to the Goldstone mode (position shift of the soliton), in which all spins rotate with the frequency of the soliton precession Ω in the laboratory frame. The presence of the rotating frame frequencies in the phenomenological description of the soliton dynamics has a simple explanation.

The frequencies (49) describe, in essence, the motion of the soliton center. Let us discuss their link with the frequencies of small oscillations, see Eq. (13). It is easy to write down expressions for the magnetization components in the laboratory coordinate frames:

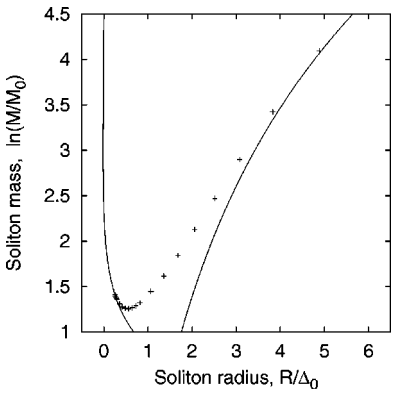

FIG. 12. The R dependence of the mass. Lines: analytical asymptotics from Eqs. (50); symbols: numerical data.

$$m_x+im_y=\Bigg[\sin\theta_0+\cos\theta_0\sum_\alpha\,(u_\alpha+v_\alpha)\cos(m\chi+\tilde{\omega}_\alpha t)$$
$$+i\sum_\alpha\,(u_\alpha-v_\alpha)\sin(m\chi+\tilde{\omega}_\alpha t)\Bigg]\cdot e^{iq\chi+i\Omega t},$$

$$m_z=\cos\theta_0-\sin\theta_0\sum_\alpha\,(u_\alpha+v_\alpha)\cos(m\chi+\tilde{\omega}_\alpha t).$$

One can see that the in-plane components have no simple frequency dependence, including the combined values $\tilde{\omega}\pm\Omega$. At the same time, the out-of-plane components m_z depend on the frequency $\tilde{\omega}$ in the rotating frame only. In our phenomenological description only the z components contain information about the position of the soliton center $\boldsymbol{X}$, determined by the condition $m_z=-1$. Thus just the frequency $\tilde{\omega}$, which is calculated above and plotted in all figures, determines the soliton motion.

The solution of the effective Eq. (47) with the nonzero frequency ω_1 allows us to calculate the effective mass of the soliton, $M=G/\omega_1$. The value of the gyroconstant is well known, $G=4\pi qA/D$, see Refs. 35 and 7. As a result, the soliton mass is finite for every soliton radius (the local mode with ω_1 exists for every R, see Fig. 3). This fact corresponds qualitatively to the calculations in Ref. 43. The soliton mass we have obtained numerically from the ω_1 data is plotted in Fig. 12 as a function of R.

In the limit of a large radius soliton the formula (23d) yields the dependence

$$M=M_0\left(\frac{R}{\Delta^0}\right)^3,\quad M_0=\frac{\hbar N_2}{D},\quad R\gg\Delta_0, \tag{50a}$$

which agrees with the results obtained in Ref. 43 and our numerical data, see Fig. 12.

In the case of small radius, $R\ll\Delta_0$, the dependence (26) is valid, thus

$$M=M_0\cdot\frac{2\omega_0}{\omega_0-\Omega}=\frac{4\pi A}{D^2}\cdot r_0^2,\quad R\ll\Delta_0, \tag{50b}$$

where r_0 was introduced in Eq. (9). This result corresponds to the one for the Belavin-Polyakov soliton,[19] $M = 4\pi A D^{-2} \cdot L^2$, because here the characteristic length r_0 is to be replaced by the system size L.

VIII. CONCLUSION

We have studied the magnon-soliton system in the model of the 2D Heisenberg easy-axis ferromagnet. Combining numerical and analytical methods, we have obtained complete results about bound and scattering magnon states in the system. A rich spectrum of truly local modes was found along with bifurcations of these modes with the change of the soliton radius. For the modes with higher azimuthal numbers m, we have verified the picture of doublets with small splitting for large soliton radii R. The spectrum changes strongly with decreasing of R: all modes with $|m|>1$ ''leave'' the region of the discrete spectrum, transforming to quasilocal modes. Such modes could be observed experimentally by soliton magnetic resonance as was done for 1D solitons.[8] Usually the magnetic resonance experiments are carried out with the saturated samples of FM, i.e., under strong enough magnetic field H along the easy axis. In this case it is convenient to watch the resonance by the field controlling. Our results were calculated without such field in order that do not encumber the text. One can see that the influence of the field H leads to the shift both frequency of the soliton precession Ω and the magnon frequency ω on the value gH, where g is the gyromagnetic relation. In the external field the soliton structure is stable in the region of frequencies: $gH<\Omega<\omega_0 + gH$.

The influence of truly local modes is important for the scattering problem, leading to the bifurcations of the phase shift. As a result, when $R<1.52\Delta_0$, the scattering picture is qualitatively the same as for the isotropic magnet which could be explained in the framework of a simple centrifugal model. There is one exception only, $m=-1$, where the local mode exists for every soliton radius.

Our investigations can be applied to the description of the eigenmodes of magnetic dots. In the present paper we develop the theory of local modes on the soliton background; it could be a good guide for the study of the normal modes in the vortex-state magnetic dots. Our theory is constructed for the soliton in the model (1), where the soliton is stabilized by the internal precession. It is clear that such a model cannot guarantee the quantitative correspondence with the case of vortex-state magnetic dots, where the static soliton structure is stabilized by the magnetic-dipole interaction. We did not consider this type of interaction in the paper, as it is difficult to account for. Nevertheless, we believe that the main features of the problem studied above are generic. First of all, we expect the appearance of modes with anomalously small frequencies, e.g., the mode of the translational oscillations of the vortex center. The nonzero frequency of this mode is caused by the interaction with the boundary only. Second, doublets with $m=\pm n$, $n>1$, should appear when the radius of the vortex is rather large.

We have used the results on the local modes for the most interesting case of the translational modes with $|m|=1$ to describe the soliton motion in the infinite-size magnet: it is possible to identify the soliton mass, which is finite due to the localized soliton structure. In contrast to both the Belavin-Polyakov soliton in the isotropic FM and the magnetic vortex in the easy-plane FM, the soliton motion in our case of the easy-axis FM is similar to the motion of a finite mass charged particle in a magnetic field.

Thus the localized precessional soliton in the easy-axis FM is an example of a 2D topological magnetic soliton with truly particlelike properties.

ACKNOWLEDGMENTS

D.D.Sh. thanks the University of Bayreuth, where part of this work was performed, for kind hospitality. Work at Kiev was partially supported by INTAS-97-31311 Grant.

*Permanent address: National Taras Shevchenko University of Kiev, 03127 Kiev, Ukraine. Electronic address: Denis_Sheka@mail.univ.kiev.ua

[1] V. L. Berezinskiĭ, Zh. Éksp. Teor. Fiz. **61**, 1145 (1972) [Sov. Phys. JETP **34**, 610 (1972)].
[2] J. M. Kosterlitz and D. J. Thouless, J. Phys. C **6**, 1181 (1973).
[3] A. A. Belavin and A. M. Polyakov, Pis'ma Zh. Éksp. Teor. Fiz. **22**, 503 (1975) [JETP Lett. **22**, 245 (1975)].
[4] J. F. Currie, J. A. Krumhansl, A. R. Bishop, and S. E. Trullinger, Phys. Rev. B **22**, 477 (1980).
[5] H. J. Mikeska and M. Steiner, Adv. Phys. **40**, 191 (1991).
[6] D. D. Wiesler, H. Zabel, and S. M. Shapiro, Z. Phys. B: Condens. Matter **93**, 277 (1994).
[7] B. A. Ivanov and A. K. Kolezhuk, Fiz. Nizk. Temp. **21**, 355 (1995) [Low Temp. Phys. **21**, 275 (1995)].
[8] J. P. Boucher, G. Rius, and Y. Henry, Europhys. Lett. **4**, 1073 (1987).
[9] F. G. Mertens, A. R. Bishop, G. M. Wysin, and C. Kawabata, Phys. Rev. Lett. **59**, 117 (1987).
[10] F. G. Mertens, A. R. Bishop, G. M. Wysin, and C. Kawabata, Phys. Rev. B **39**, 591 (1989).
[11] A. M. Kosevich, B. A. Ivanov, and A. S. Kovalev, Phys. Rep. **194**, 117 (1990).
[12] F. Waldner, J. Magn. Magn. Mater. **31-34**, 1203 (1983).
[13] F. Waldner, J. Magn. Magn. Mater. **54-57**, 873 (1986).
[14] F. Waldner, J. Magn. Magn. Mater. **104-107**, 793 (1992).
[15] C. E. Zaspel, Phys. Rev. B **48**, 926 (1993).
[16] C. E. Zaspel, T. E. Grigereit, and J. E. Drumheller, Phys. Rev. Lett. **74**, 4539 (1995).
[17] C. E. Zaspel and J. E. Drumheller, Int. J. Mod. Phys. B **10**, 3649 (1996).
[18] K. Subbaraman, C. E. Zaspel, and J. E. Drumheller, Phys. Rev. Lett. **80**, 2201 (1998).
[19] B. A. Ivanov, V. M. Muravyov, and D. D. Sheka, Zh. Éksp. Teor. Fiz. **116**, 1091 (1999) [JETP **89**, 583 (1999)].
[20] H. Walliser and G. Holzwarth, hep-ph/9907492 (unpublished).
[21] B. A. Ivanov, H. J. Schnitzer, F. G. Mertens, and G. M. Wysin, Phys. Rev. B **58**, 8464 (1998).

[22] G. M. Wysin, Phys. Rev. B **49**, 8780 (1994).
[23] G. M. Wysin and A. R. Völkel, Phys. Rev. B **54**, 12 921 (1996).
[24] A. R. Pereira, A. S. T. Pires, and M. E. Gouvêa, Phys. Lett. A **176**, 279 (1993).
[25] A. R. Pereira, A. S. T. Pires, and M. E. Gouvêa, Solid State Commun. **86**, 187 (1993).
[26] B. A. Ivanov, Pis'ma Zh. Éksp. Teor. Fiz. **61**, 898 (1995) [JETP Lett. **61**, 917 (1995)].
[27] B. A. Ivanov and V. M. Muravyov, Fiz. Nizk. Temp. **24**, 672 (1998) [Low Temp. Phys. **24**, 510 (1998)].
[28] F. K. Abdullaev, R. M. Galimzyanov, and A. S. Kirakosyan, Phys. Rev. B **60**, 6552 (1999).
[29] B. A. Ivanov, A. K. Kolezhuk, and G. M. Wysin, Phys. Rev. Lett. **76**, 511 (1996).
[30] B. Hillebrands, C. Mathieu, C. Hartmann, M. Bauer, O. Buettner, S. Riedling, B. Roos, S. O. Demokritov, B. Bartenlian, C. Chappert, D. Decanini, F. Rousseaux, E. Cambrill, A. Müller, B. Hoffmann, and U. Hartmann, J. Magn. Magn. Mater. **175**, 10 (1986).
[31] M. Grimsditch, Y. Jaccard, and I. K. Schuller, Phys. Rev. B **58**, 11 539 (1998).
[32] N. A. Usov and S. E. Peschany, J. Magn. Magn. Mater. **118**, L290 (1993).
[33] C. Mathieu, J. Jorzick, A. Frank, S. O. Demokritov, A. N. Slavin, B. Hillebrands, B. Bartenlian, C. Chappert, D. Decanini, F. Rousseaux, and E. Cambrill, Phys. Rev. Lett. **81**, 3968 (1998).
[34] K. Yu. Guslienko and A. N. Slavin, J. Appl. Phys. **87**, 6337 (2000).
[35] V. G. Bar'yakhtar and B. A. Ivanov, Sov. Sci. Rev., Sect. A **16**, 3 (1993).
[36] V. P. Voronov, B. A. Ivanov, and A. K. Kosevich, Zh. Éksp. Teor. Fiz. **84**, 2235 (1983) [Sov. Phys. JETP **84**, 2235 (1983)].
[37] B. A. Ivanov and V. A. Stephanovich, Zh. Éksp. Teor. Fiz. **91**, 638 (1986) [Sov. Phys. JETP **64**, 376 (1986)].
[38] B. A. Ivanov and A. A. Zhmudsskii, Zh. Éksp. Teor. Fiz. **115**, 1511 (1999) [JETP **88**, 833 (1999)].
[39] W. A. Harrison, *Pseudopotentials in the Theory of Metals* (Benjamin, New York, 1966).
[40] G. M. Wysin, Phys. Rev. B **54**, 15 156 (1996).
[41] F. G. Mertens, H. J. Schnitzer, and A. R. Bishop, Phys. Rev. B **56**, 2510 (1997).
[42] F. G. Mertens and A. R. Bishop, in *Nonlinear Science at the Dawn of the 21th Century*, edited by P. L. Christiansen and M. P. Soerensen (Springer-Verlag, Berlin, 1999).
[43] B. A. Ivanov and V. A. Stephanovich, Phys. Lett. A **141**, 89 (1989).